Identification of Potential Inhibitors against Attachment Glycoprotein G of Nipah Virus using Comprehensive Drug Repurposing Approach

Sangita Ghimire *ghimsangita97@gmail.com*
Department of Biotechnology,
SANN International College
(affiliated to Purbanchal University)
Kathmandu, Nepal

Sazzad Shahrear *shrszd@gmail.com*
Department of Genetic Engineering and Biotechnology
University of Dhaka,Dhaka, Bangladesh

Siddhesh Kishor Saigaonkar *siddheshsaigaonkar4@gmail.com*
Mahatma Gandhi Mission's College of Engineering and Technology
(affiliated to University ofMumbai)
Navi Mumbai, India

Laura K. Harris *oesterei@gmail.com*
Institute for Cyber-Enabled Research
Michigan State University
East Lansing, Michigan, USA

Abstract

The emerging zoonotic Nipah virus (NiV) is a major threat to public health because of its potential to cause severe outbreaks from human-to-human transmission and lack of therapeutic options currently. Identification of effective therapeutics to combat NiV infections is needed to contain future outbreaks. This research uses *in silico* methods to predict putative therapeutic candidates for the NiV attachment glycoprotein G (NiV-G) from existing therapeutic agents. To do this, virtual screening of NiV-G against 1615 FDA approved drugs publicly available from the Zinc 15 database is performed using a molecular docking approach via AutoDock Vina software. Further, a molecular dynamics simulation using WebGRO server is employed to identify top NiV-G inhibitors. Most of the binding for the top three ligands – as determined by binding energy–occurs in the catalytic groove that must contain Phe458, Trp504, Gln559, and Glu579 in order to successfully inhibit NiV-G. The molecular dynamics simulation analysis validates rigidity and stability of the docked complex through the assessment of root mean square deviations, root mean square fluctuations, solvent accessible surface area, radius of gyration, and hydrogen bond analysis from simulation trajectories. Post-molecular dynamics analysis also shows that Alvimopan, Betrixaban, and Ribociclib interact with NiV-G in the same binding pocket. Therefore, Alvimopan, Betrixaban, and Ribociclib are identified as top NiV-G inhibitors that could be used to improve NiV-infected patient outcomes when an outbreak arises.

Keywords: Nipah Virus Drug Development, Attachment Glycoprotein G, Molecular Docking, Molecular Dynamics Simulation, Drug Repurposing.

1. INTRODUCTION

Nipah virus (NiV) is a paramyxovirus that was initially found in Malaysia and Singapore in 1998–1999 during a viral encephalitis outbreak affecting pigs and humans(Chua, 2003; Chua et al., 2000). The outbreak of NiV was reported in a variety of countries on a regular basiswith a case mortality rate ranging between 50 to75%(Sharma et al., 2019; WHO, 2021a). The repeated

detection of Nipah infections in Bangladesh, India, the Philippines, and Singapore has raised serious concerns about future epidemic or pandemic outbreaks(Epstein et al., 2020; Singh et al., 2019). NiV is included as a priority disease on the World Health Organization's (WHO) research and development (R&D) Blueprint list of priority diseases(WHO, 2021b).The NiV is a zoonotic virus that is spread from animal to human by contact with the excrement or droppings of an infected animal. NiV has been documented to be transmitted in a variety of methods, including person-to-person transmission as well as food-borne transmission(S. Luby et al., 2006; S. P. Luby et al., 2009). Bats included in the genus of *Pteropus* are the natural reservoirs for the NiV(Epstein et al., 2020; Olson et al., 2002). The interaction with infected bats or even with any other intermediate hosts results in the transmission of the disease to human. The infection of NiV is associated with a wide range of clinical symptoms in human and animal(Singh et al., 2019). Severe encephalitis accompanied by fever, severe respiratory distress, nausea, and headache as well as vomiting are among the clinical manifestations of Nipah infection. In severe circumstances, some patients experienced symptoms such as pneumonia, reduced consciousness and rapid changes in behavior, among several others(Soman Pillai et al., 2020).Even thoughNiV is highly pathogenic, the consequences of Nipah infection are severe. The virus has the potential to cause a pandemic, however, no treatment protocol or therapeutic compound has been licensed to treat or prevent this virus. An effective treatment regimen is of absolute necessity against this infection.

Acute encephalitis condition is primarily managed with supportive treatment(Banerjee et al., 2019).Monoclonal antibodies and other antiviral drugs, such as Ribavirin, have been proposed as therapeutic intervention for NiV infection. A neutralizing human monoclonal antibody that is effective in a non-human primate model has been discovered and is currently undergoing clinical trials(Geisbert et al., 2014; Playford et al., 2020). Ribavirin, which has been shown to be effective against other Paramyxoviruses, has been studied in animal models and proven to be ineffective against the virus in question(Aditi & Shariff, 2019; Georges-Courbot et al., 2006).

A logical target for NiV infection therapeutic development is the glycoprotein on the envelope of most paramyxoviruses including NiV. The Nipah Glycoprotein(NiV-G) is essential for binding to the ephrin-B2 and -B3 receptors(Negrete et al., 2005, 2006). During viral entry and dissemination via cell-to-cell fusion, the fusion protein F (NiV-F) is involved in pH-independent fusion activities(Diederich et al., 2005, 2008; Erbar & Maisner, 2010). Membrane fusion is generally dependent on the coordinated actions of the NiV-G and NiV-F. Cell receptors ephrin-B2 and/or-B3 interacts with the NiV-G and responsible for its activation, causing NiV-G to undergo a conformational alteration and, as a result, activating the NiV-F fusion cascade(Aguilar et al., 2009; J. J. W. Wong et al., 2017). In order to activate and trap NiV-F, Ephrin-B2 clustering and oligomerization by NiV-G are necessary(J. J. Wong et al., 2021).Glu119–Trp125 of Ephrin-B2 and Tyr120, Pro122, Leu124 and Trp125 of Ephrin-B3 are important for Ephrin attachment with NiV-G. Among those residues, the binding of Phe120 of Ephrin (B2 and B3), at its specific binding site is found most crucial in NiV-G-Ephrin attachment(Bowden et al., 2008; Xu et al., 2008). Gln559, Glu579, Tyr581 and Ile588 of NiV-G forms the binding groove for the Phe120 of Ephrin while Leu305, Phe458 and Trp504 of Niv-G are essential for binding with the Leu124 and Trp125 of Ephrin(Bowden et al., 2008).Interfering with the interaction of NiV-G with Ephrin-B2 and/or -B3 have been proved to prevent viral entrance into the host cell by competing with both the Ephrin receptors, which are expressed on the surface of the host cell.Ephrin-B2 natural ligands and soluble Ephrin-B2 have been demonstrated to be efficacious *in vitro* (Negrete et al., 2005).

Computational approaches used to identify possible therapeutic candidates for various viral infections, specifically drug repurposing may also be useful in developing a treatment for NiVinfection targeting NiV-G.The shortening of the developmental timeline for drug discovery, reducing theeconomic burden and preclinical and clinical trials can be surpassed by the approach known as drug repurposing/repositioning.This effective approach has been used for the identification of several therapeutics including neurological disease like Alzheimer's disease, in which a drug Carmustine earlier discovered for brain cancer, can be used.Similarly, Chlorpromazine, identified for the psychiatric diseases has been used as a treatment for

Colorectal cancer(Hua et al., 2022). Thus, repurposing drugs through computational approach would reveal new treatment options for the NiV infections.

The objective of this study was to find potential entry inhibitors that will prevent the virus from infecting the host cells employing *in silico* approaches. In this paper, a deductive method has been adopted in order to identify putative drug against Nipah glycoprotein. We applied computational drug repurposing approach to NiV-G infection containment, where structure-based drug design strategy was used against the NiV-G protein, which involve the use of *in silico* pharmacophore modeling and virtual screening of lead compounds to identify potential inhibitors.NiV-G protein of Nipah virus was selected due to its primary role in viral entry and dissemination of the virus.Alvimopan, Betrixaban, and Ribociclib were found as the best lead candidate against NiV-G protein and could be a promising solution for the containment of Nipah virus infection. The outcome of this particular research can address the necessity to seek effective approach to combat the disastrous Nipah infection.

2. METHODS

2.1 Protein Structure Retrieval and Preparation

The three-dimensional structure of the NiV-G (PDB ID:3D11)(Xu et al., 2008) was retrieved from the Protein Data Bank (PDB)(Berman et al., 2000). The protein preparation was done using AutoDock tools(Morris et al., 2009).All non-protein entities attached to the crystal structure. For example, water molecules and other heteroatoms, were removed. Non-polar bonds were merged and Gasteiger charges were added during the protein preparation step using AutoDock tools.

2.2 Ligand Preparation

A set of FDA approved drugs, containing 1615 compounds, was selected for the present study for virtual screening against NiV-G. The three-dimensional structures of these FDA ligands were downloaded in structural data file (SDF) format from the ZINC 15 database(Sterling & Irwin, 2015). The compounds were filtered using DataWarrior(Sander et al., 2015) based on Lipinski's rule of five(Lipinski et al., 2001) and the compounds with appropriate pharmacokinetic properties were selected for further analysis. Energy minimization of these selected compounds was performed using Open Babel (O'Boyle et al., 2011) available in PyRx (Dallakyan & Olson, 2015). With an intent to validate the docking approach, Ribavirin, which has been previously used as a control during *in vivo* screening of viral entry inhibitors, has been used as a control (Tang et al., 2019).

2.3 Structure-based Virtual Screening

The molecular docking of the FDA drug library against the NiV-G was performed using the AutoDock Vina tool(Trott & Olson, 2009) available atPyRx (Dallakyan & Olson, 2015). The grid generation was carried out ensuring that the residues Gln559, Glu579, Tyr581 and Ile588, as well as other adjacent residues that comprised the binding groove of Ephrin, were properly encompassed inside the given rectangular grid box. The center coordinates of the grid box were positioned as specified: X=29.283, Y=6.738and Z=89.794. The grid box has dimensions of 20.620Å, 36.349Å and 39.673Å in the X, Y and Z axes, respectively, to allow the ligand to move freely inside the binding groove of the target protein.

After molecular docking has been performed, the conformation with the lowest docked energy, obtained as a negative value in Kcal/mol was chosen. The top hits selection was done on the basis of the lowest docked energy and further selection was done based on their pharmacological activity along with their preference index (PI)**.** To calculate the PI, Equation 1 was used.

$$\mathrm{PI} = \frac{\text{Number of Hydrogendonor} + \text{Number of Hydrogen acceptor} + \text{Number of rotatable bonds}}{25}$$

The binding interactions between top identified hits and glycoprotein targets were visualized using Biovia Discovery Studio (*SYSTÈMES, D., 2016)* and LigPlot+(Laskowski & Swindells, 2011).

2.4 ADMET Prediction

All the ligands used for docking analysis in this study were previously selected based on Lipinski's rule of five(Lipinski et al., 2001). The drug-likeness properties and various pharmacokinetic and toxic properties of the identified top hits were collected from SwissADME (Daina et al., 2017) and pkCSM (Pires et al., 2015).

2.5 Molecular Simulation

To evaluate the stability of the protein while bound to a specific ligand, WebGro*(https://simlab.uams.edu*) was used to perform molecular dynamics (MD) simulations of protein-ligand complexes. WebGro is an online platform to perform fully solvated MD simulations using the GROMACS simulation package (Bekker et al., 1993). The PRODRG2 server(Schüttelkopf & van Aalten, 2004) was used to construct the ligand topology for the best-docked protein-ligand complexes. Using the SPC solvation model, the protein-ligand complex was engrossed inside a triclinic water box. In this study, the GROMOS96 43a1 force field was employed. The system was neutralized by introducing sodium and chloride ions in proportion to the total charges and the system were equilibrated using an NVT/NPT ensemble. The steepest descent algorithm (5000 steps) was used to minimize the system before performing MD. The MD simulations were performed in the presence of 0.15M NaCl at a constant temperature (300 K) and pressure (1.0 bar). The number of frames in each simulation was around 1000. The simulation was run for 100 ns. The stability of the selected complexes was analyzed using Root Mean Square Deviation(RMSD), Root Mean Square Fluctuation (RMSF), Radius of Gyration (Rg), Solvent Accessible Surface Area (SASA)and the number of H-bonds in each frame over time.

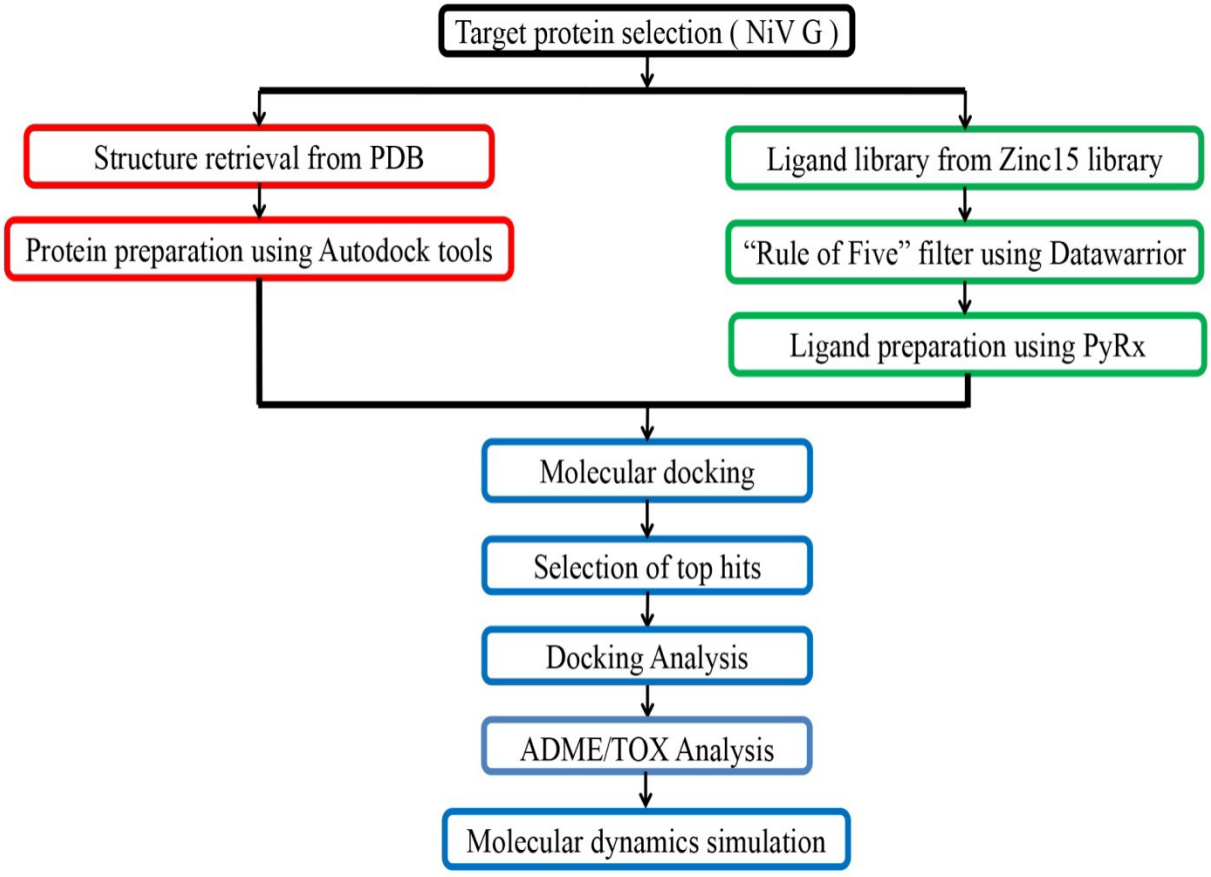

FIGURE 1: Flowchart of the Methodology of Identification of Potential Inhibitor of NipahVirus.

3. RESULTS

3.1 A total of one hundred sixty-eight compounds exhibited lowerbinding energy than the control

The molecular docking of the target protein with FDA ligands indicated several compounds will have strong interaction with NiV-G with lower binding energy. Out of 1615 FDA approved drugs, 193 ligands, that had satisfiedLipinski's rule of five, were subjected to molecular docking. The binding energy of the control Ribavirin was found to be -6.6 Kcal/mol. Out of 193 ligands being docked, 163 compounds exhibited lower binding energy than the control. The top 20 compounds were identified as top hits on the basis of the binding energy of the particular ligand with the drug target. The Preference Index(PI) was then calculated and top hits were sorted according to PI value (TABLE 1). In this study, the PI had been taken as an important parameter to prioritize the drug candidate. Moreover, the pharmacological activity of the selected top hits was also taken into consideration during candidate selection. From the top 20 hits, the top 3 hits, identified based on the PI and suitable pharmacological activity, were selected for further analysis.

No.	Compound	Hydrogen Acceptor	Hydrogen Donor	Rotatable Bonds	Binding Energy (Kcal/mol)	Preference Index	Primary Target/Activity
1	Alvimopan	6	3	8	-8.9	0.68	Peripherally acting μ-opioid receptor antagonist
2	Betrixaban	8	3	6	-8.5	0.68	Inhibitor of blood coagulating factor Xa
3	Ribociclib	9	2	5	-8.5	0.64	Inhibitor of cyclin D1/CDK4 and CDK6
4	Atenolol	5	3	8	-8.5	0.64	Cardioselectiv e beta-blocker
5	(R)-bepotastine	5	1	8	-8.6	0.56	Ophthalmic H1 antagonist
6	Dolutegravir	8	2	3	-9.3	0.52	Inhibitor of HIV-1 intergrase
7	(R)-paliperidone	7	1	4	-9.7	0.48	Atypical antipsychotic
8	Darifenacin	4	1	7	-9.5	0.48	M3 muscarinic receptor blocker
9	Deflazacort	7	1	4	-9.2	0.48	Corticosteroid

10	Triamcinolone	6	4	2	-8.8	0.48	Glucocorticoid
11	(S)-paliperidone	7	1	4	-8.8	0.48	Atypical antipsychotic
12	Acrivastine	4	1	6	-9.9	0.44	Ophthalmic H1 antagonist
13	Flunisolide	6	2	2	-8.9	0.40	Corticosteroid
14	Ziprasidone	5	1	4	-8.7	0.40	Atypical antipsychotic
15	Methylprednisolone	5	3	2	-8.6	0.40	Corticosteroid
16	Prednisolone	5	3	2	-8.6	0.40	Glucocorticoid
17	Tadalafil	7	1	1	-9.1	0.36	Inhibitor of phosphodiesterase 5
18	Desoximetasone	4	2	2	-9.1	0.32	Glucocorticoid
19	Solifenacin	4	0	3	-9.4	0.28	Muscarinic receptor antagonist
20	Esmirtazapine	3	0	0	-8.5	0.12	Inverse agonist of at H1 and 5-HT2 receptors and antagonist of α2-adrenergic receptors

TABLE 1: Drugs with Lowest Binding Energies towards NiV-G.

Among the 193 ligands, Alvimopan, Betrixaban, and Ribociclib have been selected as the top lead candidate against NiV-Gbased on their higher preference index of 0.68, 0.68, and 0.64 respectively along with lower binding energy of -8.9, -8.5, and -8.5 Kcal/mol respectively.

3.2 The selected top hits were found to be bound at the NiV-G –ephrin interaction interface

After the selection of the top 3 hits, the interaction between drug-target interfaces was visualized using Biovia Discovery Studio. It was found that the ligands were bound at the desired binding groove of the NiV-G (FIGURE 2). The interacting amino acid residues of NiV-G with the top 3 binding potential drug candidates along with the reference ligand were also analyzed (TABLE 2). The hydrophobic bonds have been analyzed with LigPlot+ and hydrogen bonds and other bonds have been analyzed with Biovia Discovery Studio.

Compound	Hydrogen Bond Residues	Hydrophobic Bond Residues	Carbon - Hydrogen bond	Binding Energy (Kcal/mol)
Alvimopan	HIS281, LYS560	ILE304, GLU505, VAL507, PRO441, TYR351, CYS282, TRP504, PHE458, TYR508, GLN559, GLY352, HIS281, LYS560, ASP302	-	-8.9
Betrixaban	CYS282	PHE458, GLN559, ASP302, TYR280, ASP219, HIS281,PRO220, PRO353, LEU221,LYS560, PRO441, TYR508, GLY506, CYS282	ASP219, PRO220	-8.5
Ribociclib	ASP2019, GLN559	GLU505, GLY506, GLN559, LYS560, PRO441, PRO353, CYS282, TYR351, GLY352, HIS281, ASP302, ASP219, PHE458, TRP504	TRP504	-8.5
Ribavirin	ASP219, HIS281, CYS282	PRO441, LYS560, PRO220, PRO353, LEU221, CYS282, HIS281, GLY352, ASP302, ASP219	ASP219	-6.6

TABLE2: Interacting Residues of Respective Top Hits with NiV-G protein.

Upon analysis of the docking poses, it was observed that Alvimopaninteracts with the residue Phe458 and Trp504 and forms hydrophobic bonds. Similarly, Betrixaban was found to interact with Phe458 while Ribociclib showed hydrophobic interaction involving residues Phe458 and Trp504 of NiV-G. These interacting residues of NiV-G are considered crucial for the interaction of NiV-G with the Leu124 and Trp125 of Ephrin. Again, Alvimopan was found to be interacting with Glu579 and Gln559, Betrixaban interacted with Gln559, and Ribociclib exhibited interaction with Gln559 residue ofNiV-G protein. These residues were responsible for forming the binding groove for Phe120 of Ephrin which is important for NiV-G-Ephrin interaction (Bowden et al., 2008).

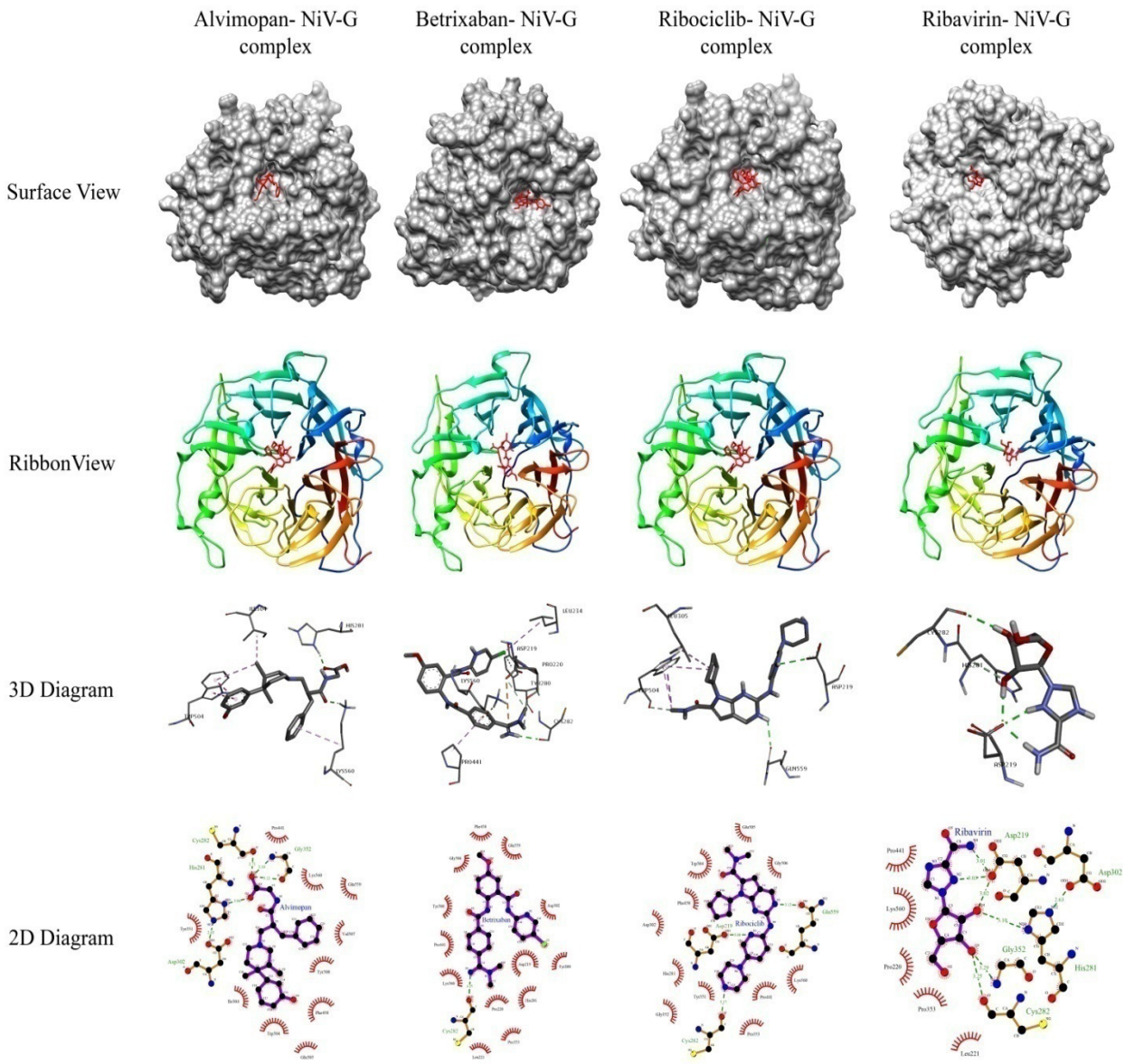

FIGURE2: Interaction Analysis Between NiV-G with Respective Top Hits at the Binding Groove: Surface view of the interaction (1st-row panel), Ribbon view of the interaction (2nd-row panel), 3D diagram of the receptor-ligand interaction at the binding site (3rd-row panel) and 2D diagram showing hydrophobic interactions (4th-row panel).

3.3 Selected drugs were found to be safe according to ADMET analysis

The FDA-approved drugswere previously filteredbased on Lipinski's Rule of five. To confirm the safety of the usage of the selected drug candidates,several properties related to absorption, distribution, metabolism, excretion, toxicity and other pharmacokinetic properties of the top 3 hits had been explored as well using SwissADMEand pkCSM server (TABLE 3).

Compound	Aqueous Solubility (log mol/L)	Blood Brain Barrier Permeability (log BB)	Human Intestinal Absorption (% Absorbed)	Total Clearance (log ml/min/kg)	Ames Toxicity	Carcinogens	Hepatotoxic	Maximum Tolerance Dose (log mg/kg/day)
Alvimopan	-3.22	-0.582	92.89	0.398	No	No	Yes	-0.101
Betrixaban	-4.71	-1.417	78.615	0.26	No	No	Yes	0.465
Ribociclib	-3.86	-1.204	94.012	0.685	No	No	Yes	-0.557

TABLE3: Interacting Residues of Respective Top Hits with NiV-G Protein.

The drug that will be absorbed has to be available in the form of a solution at the absorption site in order to achieve the desired pharmacological response (Savjani et al., 2012). Solubility is a crucial parameter to accomplish desired concentration of drug in the systemic circulation. When systemic effects are desired, drugs with poor water solubility may require high dosages to achieve therapeutic plasma concentrations after oral administration and may restrict intestinal absorption into the portal vein system (Lagorce et al., 2017). The predicted water solubility ofAlvimopan, Betrixaban and Ribociclib, obtained as the logarithm of the molar concentration (logmol/L), are -3.22, -4.71 and -3.86 respectively, suggesting that these compounds are water-soluble.

The brain endothelium forms the blood-brain barrier (BBB), which protects the central nervous system (CNS) by permitting only water and lipid-soluble molecules to pass through and selectively transport chemicals(Durán-Iturbide et al., 2020). The selected drug compounds in this study have BBB permeability less than 0.3, indicating these compounds does not readily cross the BBB. Moreover, Betrixaban and Ribociclibhave BBB permeability values less than -1, indicating their poor distribution to the brain.

Human intestine absorbance is another essential aspect of drug discovery. The amount of the drug that has entered the portal vein is used to determine human intestinal absorption(Durán-Iturbide et al., 2020). Orally given drugs must pass through the epithelium of the gastrointestinal tract in order to enter the bloodstream(Geerts & Vander Heyden, 2011). In the human intestine, compounds having an absorbance of less than 30% are thought to be poorly absorbed. Among the selected compounds, Alvimopan, and Ribociclib were predicted to be absorbed more than 90% (92.89% and 94.012 % respectively) while the absorbance for Betrixaban was predicted to be slightly lower than the previous two (78.615%).

Total clearance is a factor that influences the drug's half-life as well as its bioavailability. The total clearance influences the drug regimen as well as the dosage of the drug. It is the result of a combination of hepatic (liver and biliary) and renal clearance (Berellini et al., 2012).The total clearance values for Alvimopan, Betrixaban and Ribociclib are predicted as the value in log(ml/min/kg) with values 0.398, 0.26 and 0.685 respectively.

The Ames toxicity test is predicted in order to assess the potential mutagenic property of a compound (McCarren et al., 2011). Additionally, the potential teratogenicity and genotoxicity in the early stages of drug discovery can be evaluated with Ames toxicity (Guan et al., 2019)**.**None of the identified top compounds showed positive results on Ames toxicity indicating these possess no harmful effects.

The carcinogenicity of the compound is one major reason for the withdrawal of the many approved drugs from the market. The prediction of such property is crucial for drug discovery (Guan et al., 2019). The selected compounds were screened for their carcinogenic properties and were found to be non-carcinogenic and safe for use.

The liver plays an important role in drug metabolism and xenobiotic biotransformation. The hepatotoxic compounds may impair the normal metabolism and function of the liver, resulting in liver failure. During the development of new drugs, drug-induced liver damage has remained a key issue(Durán-Iturbide et al., 2020).All the identified top hits against target proteins were found to be hepatotoxic. However, these compounds have been approved by FDA and proved to be clinically safe after passing all trials and being used for treatment regimens for destined disease, the same can be used as inhibitors for the target protein, NiV-G, at a certain limited dose. To ensure safety after administering these drugs, the maximum tolerated dose was predicted for each compound. The maximum tolerated dose is the maximum dose of a drug that may be administered throughout chronic research without affecting the natural lifetime of the animals due to factors other than carcinogenicity (Stampfer et al., 2019).The maximum tolerated dose for Alvimopan, Betrixaban, and predicted to be -0.101, 0.465, and -0.557 (log mg/kg/day) respectively.

3.4 Identified top ligands and NiV –G protein complexes were found to be stable during MD simulation

Following the identification and validation of the safety of administering Alvimopan, Betrixaban and Ribociclib as possible Nipah entry inhibitors, MD simulations were performed using the WebGRO server to assess the stability of NiV-G protein-ligand complexes.

The RMSD value of a protein coupled to a ligand reveals how the protein backbone exists internally and evolves structurally over time in comparison to the initial point. The NiV-G was coupled to the compounds (Alvimopan, Betrixaban and Ribociclib) and RMSD profiles were created. The apo-protein (unbound NiV-G) RMSD profile was also produced and utilized as a comparative control. TheNiV-G complexed with Alvimopanas well as the NiV-G complexed with Ribociclibfollows the same pattern as the control. The RMDS pattern is somewhat slightlyhigher in NiV-G complexed with Betrixaban than in the control (Figure 3, 1st-row panel). After 40 ns, the RMSD values of the NiV-G complexed with Alvimopanand Ribociclib, as well as the apo-protein, stabilized; only the protein complexed with Betrixaban stabilized after 50 ns. All systems remain in the plateau phase for the rest of the time after stabilization. The average RMSD for NiV-G complexed with Alvimopan, Betrixaban and Ribociclib were found to be 0.2655, 0.2786 and 0.2507, respectively, whereas the average RMSD for unbound NiV-G was 0.2394.

The RMSF plots of all four systems suggest that the compounds remained bound to NiV-G protein. The fluctuation of the amino acid residues of the protein has been measured to be within 0.55 nm. In all systems, amino acid residues between 370 and 425 have fluctuated a little more than the others. The RMSF plots indicate that the binding site residues had a lower degree of fluctuation (Figure 3, 2nd-row panel).

The structural compactness and folding organization of NiV-G protein-coupled with ligands have been evaluated using SASA and Rg. During the simulation, SASA is a measurement of the surface area accessibility of the complexes, while Rg is a measure of structural compactness. SASA and Rg will most likely maintain a consistent value if the protein is folded properly; these values will fluctuate over time if a protein unfolds. SASA values for all the systems ranged from 1.6 to 1.9 nm (Figure 3, 3rd-row panel), whereas Rg values ranged from 2.02-2.1 nm (Figure 3,

4th-row panel). Both values remained relatively stable throughout time and most interestingly, the SASA and Rg values of the ligand-compound complexes followed the same pattern as the apo-protein.

The H-bond pattern analysis indicates that the ligands are constantly attached to the NiV-G protein by multiple H-bonds (FIGURE 3, 5th-row panel). When the protein-ligand complexes were analysed after the simulation, it was found that all three ligands are still interacting with certain protein residues (i.e., Gln559 and Phe458) that are crucial for Ephrin attachment (Supplementary Figure S1 and Supplementary Table 1).

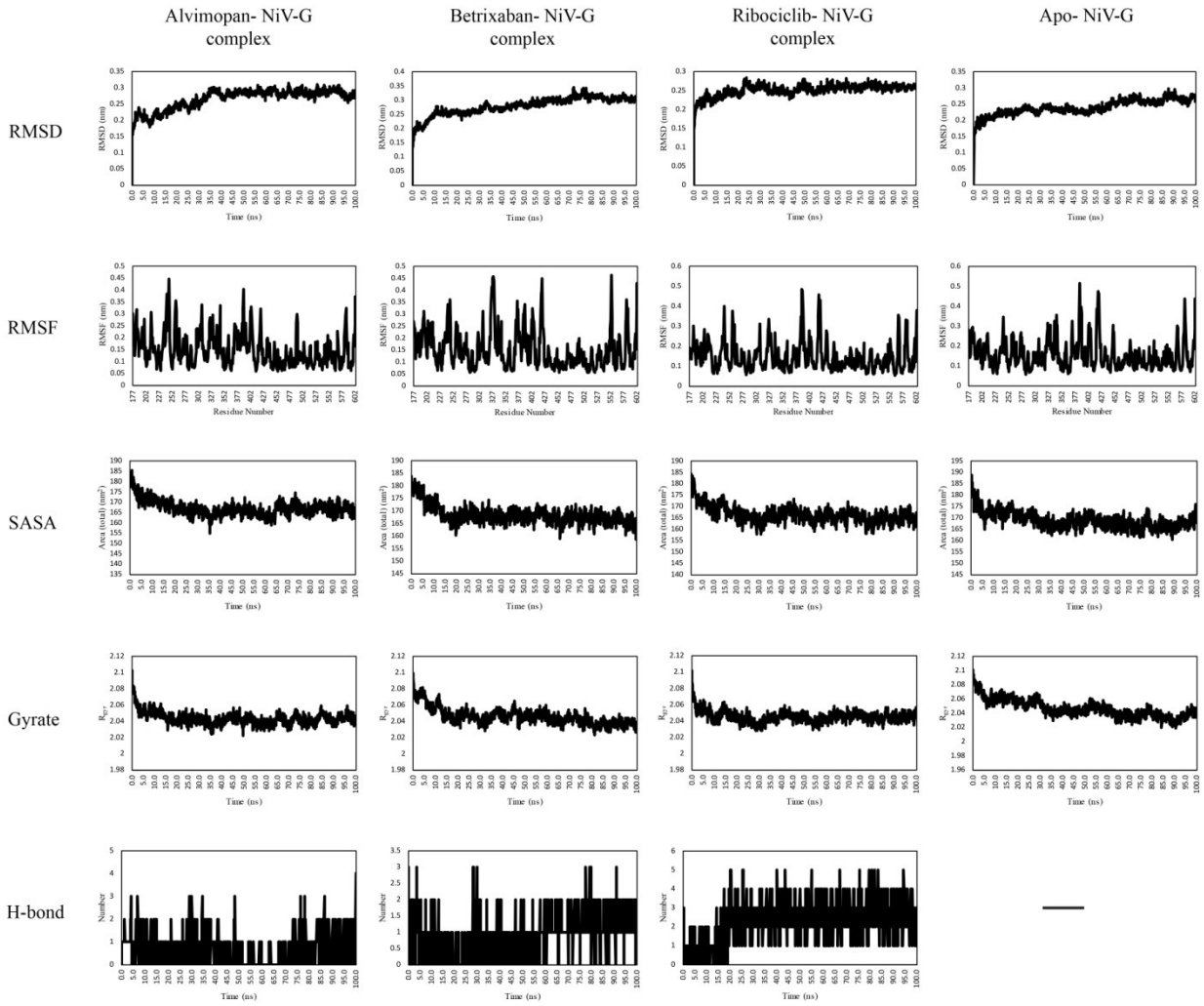

FIGURE 3: Trajectory Plots Analysis of MD Simulations: Plot of Root Mean Square Deviation (RMSD) (1st-row panel), Root Mean Square Fluctuation (RMSF) (2nd-row panel), Solvent Accessible Surface Area (SASA) (3rd-row panel), Radius of gyration (Rg) (4th-row panel) and Hydrogen bonds (5th-row panel) during MD simulation of the NiV-G protein in complex with the selected compounds (1st, 2nd and 3rd columns). The RMSD, RMSF, SASA and Rg plots of the apo-protein are shown in the 4th column.

4. DISCUSSION

To find potential entry inhibitors from the preexisting drug compounds against NiV, in this study, a computational drug repurposing approach has been utilized. FDA-approved drug compounds

were screened against the Ephrin binding groove of the NiV-G via virtual screening. FDA-approved compounds were used in this study because repurposing of drugs is a universal strategy to find out the drugs against various dreadful diseases thereby safe as ADMET tests have already been carried out for these drugs, decreasing the developmental timeline and cost, with a lower chance of failure (Kumar et al., 2019).

It was observed that163FDA-approved compounds had greater free-binding energy than the control (ribavirin) and were attached at the groove in the NiV-G protein. The top 20 hits were chosen from the 163 compounds. The top 20 hit compounds were sorted according to their preference index value (TABLE 1). To check their suitability to be used as an entry inhibitor, their pharmacological activity was checked. It was observed that the top 3 compounds have a suitable pharmacological activity to be used as entry inhibitors.

This PI was employed as a parameter to prioritize the drug candidate.PI is calculated on the basis of the number of hydrogen donors,acceptors and rotatable bonds in a particular ligand and measured within the 0 to 1 range. The higher the PI, the more suitable the compound is to be used as a drug. These three properties owe significant importance during drug development(Lipinski et al., 2001). H-bonds are widely regarded as being significant in the facilitation of protein-ligand interaction. While all other interactions remain unchanged, the potency of a compound for the specific receptor can be influenced by just one H-bond(Hamaguchi et al., 2015; Salentin et al., 2014; Sawada et al., 2010). The selected top 3 hits, Alvimopan, Betrixaban and Ribociclib, have been found to have a PI of 0.68, 0.68 and 0.64 respectively.

The analysis of docking poses of the selected hit compounds revealed that the compounds were bound at the groove of the NiV-G which is the interface of the Ephrin-NiV-G interaction. Compounds were found to form hydrophobic bonds with the Phe458 and Trp504 of NiV-G, which are important for the binding with Leu124 and Trp125 of Ephrin. Again, the selected compounds also formed hydrophobic bonds with Glu579 and Gln559, which interact with the Phe120 of Ephrin. It was previously observed that the interaction of Phe120 of Ephrin with residues NiV-G is the most crucial for the Ephrin to bind with NiV-G (Bowden et al., 2008). Based on these findings, it is reasonable to assume that these compounds will block Ephrin-NiV-G interaction.

To ensure the safety of utilizing the selected compounds, ADMET analysis of these compounds was performed, as well as the usage of these compounds was also checked. According to the ADMET analysis, all three compounds are soluble in water but not permeable to the blood-brain barrier (BBB). Furthermore, none were determined to be carcinogenic or toxic. Although the compounds were predicted to be hepatotoxic, their hepatotoxicity can be minimized by administering them at the maximum tolerated dose.Alvimopan is an orally administered, peripherally acting μ opioid antagonist. Although the oral bioavailability is low (7%), because of the high affinity for the peripheral μ-receptor in the gastrointestinal tract, 80% to 90% of systemically accessible Alvimopan can bind to plasma protein. Betrixaban is an anticoagulant that is also administered orally. It has a higher oral bioavailability (34%) than Alvimopan while only 60% of systemically accessible Betrixaban can bind to plasma protein(Wishart et al., 2018). Ribociclib is a cyclin-dependent kinase 4 and 6 (CDK4/6) inhibitor that is used to treat many forms of breast cancer. The oral bioavailability of the drug is still being investigated but it has been reported that 70% of systemically accessible Ribociclib can bind to plasma protein(Agency, n.d.). Because all three drugs have a stronger propensity to attach to serum proteins, it is indeed possible that they will also bind to the NiV G protein, which is freely circulating in the serum of the infected patient.

After validating the safety of using the selected compounds as possible entry inhibitors, MD simulation was carried out to gain a better understanding of the behavior of the molecular interactions of the NiV-G protein with the ligands in their dynamics state. Following the binding of the ligands, the MD simulation analysis generated significant data on the fluctuation, structural and conformational changes of NiV-G protein, as well as the inter-atomic or intra-atomic

interactions, for a period of 100 ns. RMSD, RMSF, SASA, Rg and H-bond plots were derived from the MD simulated trajectories and evaluated to confirm the stability of each NiV-G protein-ligand complex.

The lower RMSD values of NiV-G protein backbone atoms, whether coupled with the ligands or not, suggest that all systems remained stable during the MD simulation and binding of the selected ligands does not affect the structural stability of the protein. The RMSF plots show a lower fluctuation at the binding site residues, indicating that the ligands will remain attached to those residues constantly. SASA and Rg values were constant throughout time as well. The SASA and Rg values of all the systems, interestingly, tend to decrease over time, demonstrating the structural compactness of the systems. The H-bonds plots and post-simulation snapshot analysis suggest that the ligands remained attached to the active site pocket with multiple H-bonds along with other types of bonds throughout time. These findings suggest that the selected three compounds (Alvimopan, Betrixaban andRibociclib) will remain tightly attached to the protein and will inhibit the attachment of the NiV-G protein with Ephrin, therefore preventing the Nipah virus from infecting host cells.

During the COVID-19 pandemic, drug repurposing was used to establish a successful treatment option. Several FDA-approved drugs were subjected to clinical trials(Sultana et al., 2020). In vitro studies also suggested that FDA-approved drugs could be used to treat COVID-19(Jang et al., 2021). So, in this study, we used the drug repurposing strategy to find an effective inhibitor that can inhibit NiV-G binding to Ephrin.

Despite the fact that NiV is an emerging paramyxovirus and that evidence of recurring outbreaks of this virus is being documented, there is not yet an available therapeutic approach that is proven to be effective.Employing a molecular drug docking approach, FDA approved ligands were used in this study to identify potential NiV-G inhibitors. In spite of the fact that there areplethora of benefits to drug repositioning in comparison to the more conventional de novo strategy, it is not always effective. To validate the inhibitory effects of these compounds against NiV-G in order for them to be considered as prospective therapeutics for NiV infection, extensive laboratory and clinical trials are required.

5. CONCLUSION

An effective therapeutics is of utmost necessity to combat NiV infections, a global threat to contain future outbreaks. Despite the urgent requirement for an effective therapeutic option against NiV and the fact that the virus has already caused multiple epidemics in Asian countries, still there is currently no such drug available. The drug repurposing strategy was utilized in this study with the objective of identifying potential NiV inhibitors. Alvimopan, Betrixaban, and Ribociclib have been identified as potential inhibitors of NiV through the application of molecular docking as well as virtual screening approaches.Theplotted interactions of candidate drugs bound with the NiV-G protein would aid in the choice of the appropriate drugs.In order to cross-validate the results of the molecular docking and screening, MD simulation was carried out. This simulation validated the stability of the ligand-bound NiV-G complex for the candidates that were identified through this study.The identified drugs can be employed in treating the Nipah outbreak for which effective medicationhave been yet discovered or prescribed.Despite the limitations of computational docking approach, it was used to identify possible drug candidates.The repurposing of the drugs that have already been approved for human use for other diseases can be an option for emergency use upon approval from the regulatory bodies, if subsequent outbreak occurs in the future, leading for the practical safe implications of the FDA approved drugs. Extensive laboratory and clinical studies are required to validate the inhibitory potential of these candidates against NiV-G as possible NiV therapeutics.

6. ACKNOWLEDGEMENT

The authors acknowledge the support from Darwin International Conference, 2020 for the assistance in formulating the research idea.

7. ORCHID

Sangita Ghimire https://orcid.org/0000-0001-6085-2959
Sazzad Shahrear https://orcid.org/0000-0003-3278-3110
Siddhesh Saigaonkar https://orcid.org/0000-0002-7193-6506

8. CONFLICT OF INTEREST

All authors declared that they have no conflict of interest.

9. FUNDING

The project was not funded by any internal or external organization.

10. AVAILABILITY OF DATA

The data underlying this article are available in the article and its online supplementary material.

11. REFERENCES

Aditi, & Shariff, M. (2019). Nipah virus infection: A review. *Epidemiology and Infection*, *147*, e95. https://doi.org/10.1017/S0950268819000086

Agency, E. M. (n.d.). *Kisqali: EPAR – Product Information*. https://www.ema.europa.eu/en/documents/product-information/kisqali-epar-product-information_en.pdf

Aguilar, H. C., Ataman, Z. A., Aspericueta, V., Fang, A. Q., Stroud, M., Negrete, O. A., Kammerer, R. A., & Lee, B. (2009). A Novel Receptor-induced Activation Site in the Nipah Virus Attachment Glycoprotein (G) Involved in Triggering the Fusion Glycoprotein (F). *Journal of Biological Chemistry*, *284*(3), 1628–1635. https://doi.org/10.1074/jbc.M807469200

Banerjee, S., Gupta, N., Kodan, P., Mittal, A., Ray, Y., Nischal, N., Soneja, M., Biswas, A., & Wig, N. (2019). Nipah virus disease: A rare and intractable disease. *Intractable & Rare Diseases Research*, *8*(1), 1–8. https://doi.org/10.5582/irdr.2018.01130

Bekker, H., J C Berendsen, H., van Drunen, R., van der Spoel, D., Sijbers, A., Keegstra, H., Reitsma, B., Renardus, M. K. R., Achterop, S., & Dijkstra, E. J. (1993). Gromacs : A parallel computer for molecular dynamics simulations. *Physics Computing*, 252–256.

Berellini, G., Waters, N. J., & Lombardo, F. (2012). In silico Prediction of Total Human Plasma Clearance. *Journal of Chemical Information and Modeling*, *52*(8), 2069–2078. https://doi.org/10.1021/ci300155y

Berman, H. M., Westbrook, J., Feng, Z., Gilliland, G., Bhat, T. N., Weissig, H., Shindyalov, I. N., & Bourne, P. E. (2000). The Protein Data Bank. In *Nucleic Acids Research* (Vol. 28, Issue 1, pp. 235–242). Oxford University Press. https://doi.org/10.1093/nar/28.1.235

Bowden, T. A., Aricescu, A. R., Gilbert, R. J. C., Grimes, J. M., Jones, E. Y., & Stuart, D. I. (2008). Structural basis of Nipah and Hendra virus attachment to their cell-surface receptor ephrin-B2. *Nature Structural & Molecular Biology*, *15*(6), 567–572. https://doi.org/10.1038/nsmb.1435

Chua, K. B. (2003). Nipah virus outbreak in Malaysia. *Journal of Clinical Virology*, *26*(3), 265–275. https://doi.org/10.1016/S1386-6532(02)00268-8

Chua, K. B., Bellini, W. J., Rota, P. A., Harcourt, B. H., Tamin, A., Lam, S. K., Ksiazek, T. G., Rollin, P. E., Zaki, S. R., Shieh, W.-J., Goldsmith, C. S., Gubler, D. J., Roehrig, J. T., Eaton, B., Gould, A. R., Olson, J., Field, H., Daniels, P., Ling, A. E., … Mahy, B. W. J. (2000). Nipah Virus: A Recently Emergent Deadly Paramyxovirus. *Science*, *288*(5470), 1432–1435.

https://doi.org/10.1126/science.288.5470.1432

Daina, A., Michielin, O., & Zoete, V. (2017). SwissADME: a free web tool to evaluate pharmacokinetics, drug-likeness and medicinal chemistry friendliness of small molecules. *Scientific Reports*, *7*(1), 42717. https://doi.org/10.1038/srep42717

Dallakyan, S., & Olson, A. J. (2015). *Small-Molecule Library Screening by Docking with PyRx* (pp. 243–250). https://doi.org/10.1007/978-1-4939-2269-7_19

Diederich, S., Moll, M., Klenk, H.-D., & Maisner, A. (2005). The Nipah Virus Fusion Protein Is Cleaved within the Endosomal Compartment. *Journal of Biological Chemistry*, *280*(33), 29899–29903. https://doi.org/10.1074/jbc.M504598200

Diederich, S., Thiel, L., & Maisner, A. (2008). Role of endocytosis and cathepsin-mediated activation in Nipah virus entry. *Virology*, *375*(2), 391–400. https://doi.org/10.1016/j.virol.2008.02.019

Durán-Iturbide, N. A., Díaz-Eufracio, B. I., & Medina-Franco, J. L. (2020). In Silico ADME/Tox Profiling of Natural Products: A Focus on BIOFACQUIM. *ACS Omega*, *5*(26), 16076–16084. https://doi.org/10.1021/acsomega.0c01581

Epstein, J. H., Anthony, S. J., Islam, A., Kilpatrick, A. M., Ali Khan, S., Balkey, M. D., Ross, N., Smith, I., Zambrana-Torrelio, C., Tao, Y., Islam, A., Quan, P. L., Olival, K. J., Khan, M. S. U., Gurley, E. S., Hossein, M. J., Field, H. E., Fielder, M. D., Briese, T., … Daszak, P. (2020). Nipah virus dynamics in bats and implications for spillover to humans. *Proceedings of the National Academy of Sciences*, *117*(46), 29190–29201. https://doi.org/10.1073/pnas.2000429117

Erbar, S., & Maisner, A. (2010). Nipah virus infection and glycoprotein targeting in endothelial cells. *Virology Journal*, *7*(1), 305. https://doi.org/10.1186/1743-422X-7-305

Geerts, T., & Vander Heyden, Y. (2011). In Silico Predictions of ADME-Tox Properties: Drug Absorption. *Combinatorial Chemistry & High Throughput Screening*, *14*(5), 339–361. https://doi.org/10.2174/138620711795508359

Geisbert, T. W., Mire, C. E., Geisbert, J. B., Chan, Y.-P., Agans, K. N., Feldmann, F., Fenton, K. A., Zhu, Z., Dimitrov, D. S., Scott, D. P., Bossart, K. N., Feldmann, H., & Broder, C. C. (2014). Therapeutic Treatment of Nipah Virus Infection in Nonhuman Primates with a Neutralizing Human Monoclonal Antibody. *Science Translational Medicine*, *6*(242). https://doi.org/10.1126/scitranslmed.3008929

Georges-Courbot, M. C., Contamin, H., Faure, C., Loth, P., Baize, S., Leyssen, P., Neyts, J., & Deubel, V. (2006). Poly(I)-Poly(C 12 U) but Not Ribavirin Prevents Death in a Hamster Model of Nipah Virus Infection. *Antimicrobial Agents and Chemotherapy*, *50*(5), 1768–1772. https://doi.org/10.1128/AAC.50.5.1768-1772.2006

Guan, L., Yang, H., Cai, Y., Sun, L., Di, P., Li, W., Liu, G., & Tang, Y. (2019). ADMET-score – a comprehensive scoring function for evaluation of chemical drug-likeness. *MedChemComm*, *10*(1), 148–157. https://doi.org/10.1039/C8MD00472B

Hamaguchi, W., Masuda, N., Miyamoto, S., Shiina, Y., Kikuchi, S., Mihara, T., Moriguchi, H., Fushiki, H., Murakami, Y., Amano, Y., Honbou, K., & Hattori, K. (2015). Synthesis, SAR study, and biological evaluation of novel quinoline derivatives as phosphodiesterase 10A inhibitors with reduced CYP3A4 inhibition. *Bioorganic & Medicinal Chemistry*, *23*(2), 297–313. https://doi.org/10.1016/j.bmc.2014.11.039

Hua, Y., Dai, X., Xu, Y., Xing, G., Liu, H., Lu, T., Chen, Y., & Zhang, Y. (2022). Drug repositioning: Progress and challenges in drug discovery for various diseases. *European Journal of Medicinal Chemistry*, *234*, 114239. https://doi.org/10.1016/j.ejmech.2022.114239

Jang, W. D., Jeon, S., Kim, S., & Lee, S. Y. (2021). Drugs repurposed for COVID-19 by virtual screening of 6,218 drugs and cell-based assay. *Proceedings of the National Academy of Sciences*, *118*(30). https://doi.org/10.1073/pnas.2024302118

Kumar, R., Harilal, S., Gupta, S. V., Jose, J., Thomas Parambi, D. G., Uddin, M. S., Shah, M. A., & Mathew, B. (2019). Exploring the new horizons of drug repurposing: A vital tool for turning hard work into smart work. *European Journal of Medicinal Chemistry*, *182*, 111602. https://doi.org/10.1016/j.ejmech.2019.111602

Lagorce, D., Douguet, D., Miteva, M. A., & Villoutreix, B. O. (2017). Computational analysis of calculated physicochemical and ADMET properties of protein-protein interaction inhibitors. *Scientific Reports*, *7*(1), 46277. https://doi.org/10.1038/srep46277

Laskowski, R. A., & Swindells, M. B. (2011). LigPlot+: Multiple Ligand–Protein Interaction Diagrams for Drug Discovery. *Journal of Chemical Information and Modeling*, *51*(10), 2778–2786. https://doi.org/10.1021/ci200227u

Lipinski, C. A., Lombardo, F., Dominy, B. W., & Feeney, P. J. (2001). Experimental and computational approaches to estimate solubility and permeability in drug discovery and development settings 1PII of original article: S0169-409X(96)00423-1. The article was originally published in Advanced Drug Delivery Reviews 23 (1997). *Advanced Drug Delivery Reviews*, *46*(1–3), 3–26. https://doi.org/10.1016/S0169-409X(00)00129-0

Luby, S. P., Gurley, E. S., & Hossain, M. J. (2009). Transmission of Human Infection with Nipah Virus. *Clinical Infectious Diseases*, *49*(11), 1743–1748. https://doi.org/10.1086/647951

Luby, S., Rahman, M., Hossain, M., Blum, L., Husain, M., Gurley, E., Khan, R., Ahmed, B.-N., Rahman, S., Nahar, N., Kenah, E., Comer, J., & Ksiazek, T. (2006). Foodborne Transmission of Nipah Virus, Bangladesh. *Emerging Infectious Diseases*, *12*(12), 1888–1894. https://doi.org/10.3201/eid1212.060732

McCarren, P., Springer, C., & Whitehead, L. (2011). An investigation into pharmaceutically relevant mutagenicity data and the influence on Ames predictive potential. *Journal of Cheminformatics*, *3*(1), 51. https://doi.org/10.1186/1758-2946-3-51

Morris, G. M., Huey, R., Lindstrom, W., Sanner, M. F., Belew, R. K., Goodsell, D. S., & Olson, A. J. (2009). AutoDock4 and AutoDockTools4: Automated docking with selective receptor flexibility. *Journal of Computational Chemistry*, *30*(16), 2785–2791. https://doi.org/10.1002/jcc.21256

Negrete, O. A., Levroney, E. L., Aguilar, H. C., Bertolotti-Ciarlet, A., Nazarian, R., Tajyar, S., & Lee, B. (2005). EphrinB2 is the entry receptor for Nipah virus, an emergent deadly paramyxovirus. *Nature*, *436*(7049), 401–405. https://doi.org/10.1038/nature03838

Negrete, O. A., Wolf, M. C., Aguilar, H. C., Enterlein, S., Wang, W., Mühlberger, E., Su, S. V, Bertolotti-Ciarlet, A., Flick, R., & Lee, B. (2006). Two Key Residues in EphrinB3 Are Critical for Its Use as an Alternative Receptor for Nipah Virus. *PLoS Pathogens*, *2*(2), e7. https://doi.org/10.1371/journal.ppat.0020007

O'Boyle, N. M., Banck, M., James, C. A., Morley, C., Vandermeersch, T., & Hutchison, G. R. (2011). Open Babel: An open chemical toolbox. *Journal of Cheminformatics*, *3*(1), 33. https://doi.org/10.1186/1758-2946-3-33

Olson, J. G., Rupprecht, C., Rollin, P. E., An, U. S., Niezgoda, M., Clemins, T., Walston, J., & Ksiazek, T. G. (2002). Antibodies to Nipah-Like Virus in Bats (Pteropus lylei) , Cambodia. *Emerging Infectious Diseases*, *8*(9), 987–988. https://doi.org/10.3201/eid0809.010515

Pires, D. E. V., Blundell, T. L., & Ascher, D. B. (2015). pkCSM: Predicting small-molecule pharmacokinetic and toxicity properties using graph-based signatures. *Journal of Medicinal*

Chemistry, *58*(9), 4066–4072. https://doi.org/10.1021/acs.jmedchem.5b00104

Playford, E. G., Munro, T., Mahler, S. M., Elliott, S., Gerometta, M., Hoger, K. L., Jones, M. L., Griffin, P., Lynch, K. D., Carroll, H., El Saadi, D., Gilmour, M. E., Hughes, B., Hughes, K., Huang, E., de Bakker, C., Klein, R., Scher, M. G., Smith, I. L., … Broder, C. C. (2020). Safety, tolerability, pharmacokinetics, and immunogenicity of a human monoclonal antibody targeting the G glycoprotein of henipaviruses in healthy adults: a first-in-human, randomised, controlled, phase 1 study. *The Lancet Infectious Diseases*, *20*(4), 445–454. https://doi.org/10.1016/S1473-3099(19)30634-6

Salentin, S., Haupt, V. J., Daminelli, S., & Schroeder, M. (2014). Polypharmacology rescored: Protein–ligand interaction profiles for remote binding site similarity assessment. *Progress in Biophysics and Molecular Biology*, *116*(2–3), 174–186. https://doi.org/10.1016/j.pbiomolbio.2014.05.006

Sander, T., Freyss, J., Von Korff, M., & Rufener, C. (2015). DataWarrior: An open-source program for chemistry aware data visualization and analysis. *Journal of Chemical Information and Modeling*, *55*(2), 460–473. https://doi.org/10.1021/ci500588j

Savjani, K. T., Gajjar, A. K., & Savjani, J. K. (2012). Drug Solubility: Importance and Enhancement Techniques. *ISRN Pharmaceutics*, *2012*, 1–10. https://doi.org/10.5402/2012/195727

Sawada, T., Fedorov, D. G., & Kitaura, K. (2010). Role of the Key Mutation in the Selective Binding of Avian and Human Influenza Hemagglutinin to Sialosides Revealed by Quantum-Mechanical Calculations. *Journal of the American Chemical Society*, *132*(47), 16862–16872. https://doi.org/10.1021/ja105051e

Schüttelkopf, A. W., & van Aalten, D. M. F. (2004). PRODRG : a tool for high-throughput crystallography of protein–ligand complexes. *Acta Crystallographica Section D Biological Crystallography*, *60*(8), 1355–1363. https://doi.org/10.1107/S0907444904011679

Sharma, V., Kaushik, S., Kumar, R., Yadav, J. P., & Kaushik, S. (2019). Emerging trends of Nipah virus: A review. *Reviews in Medical Virology*, *29*(1), e2010. https://doi.org/10.1002/rmv.2010

Singh, R. K., Dhama, K., Chakraborty, S., Tiwari, R., Natesan, S., Khandia, R., Munjal, A., Vora, K. S., Latheef, S. K., Karthik, K., Singh Malik, Y., Singh, R., Chaicumpa, W., & Mourya, D. T. (2019). Nipah virus: epidemiology, pathology, immunobiology and advances in diagnosis, vaccine designing and control strategies – a comprehensive review. *Veterinary Quarterly*, *39*(1), 26–55. https://doi.org/10.1080/01652176.2019.1580827

Soman Pillai, V., Krishna, G., & Valiya Veettil, M. (2020). Nipah Virus: Past Outbreaks and Future Containment. *Viruses*, *12*(4), 465. https://doi.org/10.3390/v12040465

Stampfer, H. G., Gabb, G. M., & Dimmitt, S. B. (2019). Why maximum tolerated dose? *British Journal of Clinical Pharmacology*, *85*(10), 2213–2217. https://doi.org/10.1111/bcp.14032

Sterling, T., & Irwin, J. J. (2015). ZINC 15 - Ligand Discovery for Everyone. *Journal of Chemical Information and Modeling*, *55*(11), 2324–2337. https://doi.org/10.1021/acs.jcim.5b00559

Sultana, J., Crisafulli, S., Gabbay, F., Lynn, E., Shakir, S., & Trifirò, G. (2020). Challenges for Drug Repurposing in the COVID-19 Pandemic Era. *Frontiers in Pharmacology*, *11*. https://doi.org/10.3389/fphar.2020.588654

SYSTÈMES, D. (2016). BIOVIA Discovery Studio Dassault Syst mes BIOVIA, Discovery Studio Modeling Environment, Release 2017. Dassault Syst mes. (n.d.).

Tang, W., Li, M., Liu, Y., Liang, N., Yang, Z., Zhao, Y., Wu, S., Lu, S., Li, Y., & Liu, F. (2019). Small molecule inhibits respiratory syncytial virus entry and infection by blocking the interaction of the viral fusion protein with the cell membrane. *The FASEB Journal*, *33*(3), 4287–4299. https://doi.org/10.1096/fj.201800579R

Trott, O., & Olson, A. J. (2009). AutoDock Vina: Improving the speed and accuracy of docking with a new scoring function, efficient optimization, and multithreading. *Journal of Computational Chemistry*, NA-NA. https://doi.org/10.1002/jcc.21334

WebGRO for Macromolecular Simulations (https://simlab.uams.edu/). (n.d.).

WHO. (n.d.). *Morbidity and mortality due to Nipah or Nipah-like virus encephalitis in WHO South-East Asia Region, 2001-2018*. https://www.google.com/search?q=Morbidity+and+mortality+due+to+Nipah+or+Nipah-like+virus+encephalitis+in+WHO+South-East+Asia+Region%2C+2001-2018&oq=Morbidity+and+mortality+due+to+Nipah+or+Nipah-like+virus+encephalitis+in+WHO+South-East+Asia+Region%2C+2001

WHO. (2021a). *Nipah virus disease - India*. https://www.who.int/emergencies/disease-outbreak-news/item/nipah-virus-disease---india

WHO. (2021b). *Prioritizing diseases for research and development in emergency contexts*. https://www.who.int/activities/prioritizing-diseases-for-research-and-development-in-emergency-contexts

Wishart, D. S., Feunang, Y. D., Guo, A. C., Lo, E. J., Marcu, A., Grant, J. R., Sajed, T., Johnson, D., Li, C., Sayeeda, Z., Assempour, N., Iynkkaran, I., Liu, Y., Maciejewski, A., Gale, N., Wilson, A., Chin, L., Cummings, R., Le, D., … Wilson, M. (2018). DrugBank 5.0: a major update to the DrugBank database for 2018. *Nucleic Acids Research*, *46*(D1), D1074–D1082. https://doi.org/10.1093/nar/gkx1037

Wong, J. J., Chen, Z., Chung, J. K., Groves, J. T., & Jardetzky, T. S. (2021). EphrinB2 clustering by Nipah virus G is required to activate and trap F intermediates at supported lipid bilayer–cell interfaces. *Science Advances*, *7*(5). https://doi.org/10.1126/sciadv.abe1235

Wong, J. J. W., Young, T. A., Zhang, J., Liu, S., Leser, G. P., Komives, E. A., Lamb, R. A., Zhou, Z. H., Salafsky, J., & Jardetzky, T. S. (2017). Monomeric ephrinB2 binding induces allosteric changes in Nipah virus G that precede its full activation. *Nature Communications*, *8*(1), 781. https://doi.org/10.1038/s41467-017-00863-3

Xu, K., Rajashankar, K. R., Chan, Y. P., Himanen, J. P., Broder, C. C., & Nikolov, D. B. (2008). Host cell recognition by the henipaviruses: Crystal structures of the Nipah G attachment glycoprotein and its complex with ephrin-B3. *Proceedings of the National Academy of Sciences of the United States of America*, *105*(29), 9953–9958. https://doi.org/10.1073/pnas.0804797105

SUPPLEMENTARY FILES

Supplementary figure 1: Post simulation interaction analysis between NiV-G with respective top hits at the binding groove.

Supplementary Table 1: Post simulation interaction analysis between top hits andNiV-G receptor.

Supplementary File

Supplementary figure 1: Post simulation interaction analysis between NiV-G with respective top hits at the binding groove: Surface view of the interaction (1st-row panel),

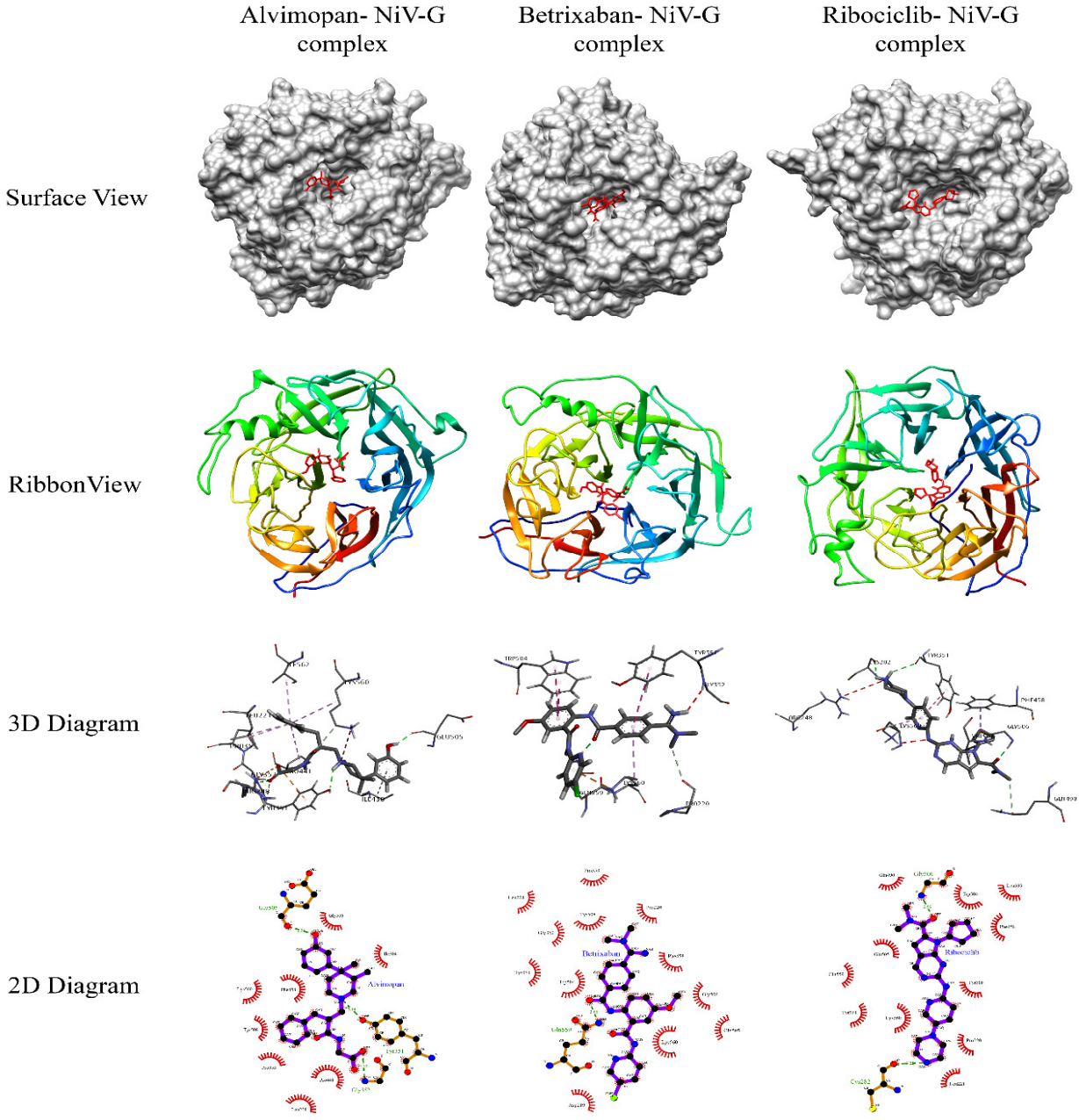

Ribbon view of the interaction (2nd-row panel), 3D diagram of the receptor-ligand interaction at the binding site (3rd-row panel) and 2D diagram showing hydrophobic interactions (4th-row panel).

Supplementary Table 1: Post simulation interaction analysis between top hits and NiV-G receptor.

Compound	Hydrogen Bond Residues	Hydrophobic Bond	Carbon - Hydrogen bond
Alvimopan	Tyr351, Glu505, Gly 352	Glu505, Gly506, Ile304, Lys560, Phe458, Tyr508, Pro353, Pro441, Tyr351, Gly352, Leu221	Lys560, Tyr351
Betrixaban	Gln559	Pro353, Leu221, Tyr508, Gly352, Pro220, Tyr351, Trp504, Phe458, Gln559, Gly506, Lys560, Glu505, Asp219	Pro220
Ribociclib	Gly506, Tyr351, Cys282	Gln490, Gly506, Trp504, Leu305, Phe458, Glu505, Gln559, Tyr508, Tyr351, Lys560, Pro220, Cys282, Leu221	Gln490